JOURNAL OF GUIDANCE, CONTROL, AND DYNAMICS
Vol. 24, No. 5, September–October 2001

Precision of Satellite Laser Ranging Calibration of the Naval Space Surveillance System

Paul W. Schumacher, Jr.*
Naval Space Command, Dahlgren, Virginia 22448-5300
G. Charmaine Gilbreath†
Naval Research Laboratory, Washington, D.C. 20375
Mark A. Davis‡
Honeywell Technical Solutions, Inc., Lanham, Maryland 20706
and
Edward D. Lydick§
Naval Space Command, Dahlgren, Virginia 22448-5300

The Naval Space Surveillance System is a network of radio frequency interferometer stations designed to detect satellites. Angular metric data from the system are used in real time to update the catalog of known space objects maintained by the U.S. Air Force and Naval components of United States Space Command. For many years the system has operated with a near real-time calibration of the detector electronics but without a rigorous tie to an external reference frame. One way to establish such a tie is by comparing system measurements with data derived by satellite laser ranging. In principle, public-domain laser ranging data on geodetic satellites can always be used to generate a few high-precision reference orbits whose ephemerides can be compared with surveillance measurements. In the right circumstances special laser tracking data on any suitable satellite can be taken simultaneously with surveillance measurements and compared directly. Both approaches offer benefit to space surveillance operations, and both have been demonstrated in previous work. This analysis initiates the analytical investigation of how precisely errors can be resolved in the surveillance measurements, using laser ranging derived data. Equations are presented, which relate Naval space surveillance uncertainties to reference data uncertainties in explicit terms. Simple geometric measurement models are considered, rather than detailed physical measurement models, in order to provide fundamental understanding of how errors transform in the two types of calibration considered. The resulting formulas are suitable for deriving calibration requirements and simplified error budgets, either analytically or by numerical simulation.

Nomenclature

A	=	azimuth of surveillance station measurement frame
A_R	=	satellite laser-ranging (SLR) receiver telescope area
c	=	speed of light
$\boldsymbol{E}_c$	=	local east unit vector at calibration station
$\boldsymbol{E}_s$	=	local east unit vector at surveillance station
$\boldsymbol{E}'_s$	=	local east unit vector in surveillance measurement frame
E_0	=	energy in transmitted laser pulse
e	=	eccentricity of geodetic reference ellipsoid; also, base of natural logarithms
G_T	=	SLR transmitter gain
G^*_T	=	optimum SLR transmitter gain
$\boldsymbol{H}_c$	=	geodetic local vertical unit vector at calibration station
$\boldsymbol{H}_s$	=	geodetic local vertical unit vector at surveillance station
$\boldsymbol{H}'_s$	=	local vertical unit vector in surveillance measurement frame
h	=	Planck's constant
K	=	proportionality constant in simultaneous-track variance relation
$\boldsymbol{k}$	=	north polar unit vector
m	=	east–west direction cosine in surveillance measurement frame
$\boldsymbol{N}_c$	=	local north unit vector at calibration station
N_{pe}	=	number of photoelectrons available in laser-ranging detector
$\boldsymbol{N}_s$	=	local north unit vector at surveillance station
$\boldsymbol{N}'_s$	=	local north unit vector in surveillance measurement frame
n	=	north–south direction cosine in surveillance measurement frame
$\boldsymbol{R}_c$	=	calibration station position
R_s	=	distance from geocenter to surveillance station position
$\boldsymbol{R}_s$	=	surveillance station position, $(X_s, Y_s, Z_s)^T$
$\boldsymbol{r}$	=	satellite position, $(x, y, z)^T$
T_a	=	SLR one-way atmospheric transmission factor
T_c	=	SLR one-way cirrus cloud transmission factor
t	=	observation time at surveillance station
$\boldsymbol{u}_c$	=	line-of-sight unit vector from calibration station to satellite
$\boldsymbol{u}_s$	=	line-of-sight unit vector from surveillance station to satellite
δE	=	nominal position uncertainty in satellite reference ephemeris
δm	=	uncertainty in surveillance east–west direction cosine
δn	=	uncertainty in surveillance north–south direction cosine
δS	=	nominal position uncertainty in surveillance station location
$\delta\beta$	=	nominal surveillance direction-cosine uncertainty
$\delta\varepsilon$	=	uncertainty in SLR-measured elevation angle
$\delta\Theta$	=	SLR total angular measurement uncertainty
$\delta\theta$	=	nominal SLR boresight pointing uncertainty (jitter)
$\delta\psi$	=	uncertainty in SLR-measured azimuth
ε	=	elevation angle of satellite at calibration station

Received 20 July 1999; revision received 10 November 2000; accepted for publication 27 November 2000. This material is declared a work of the U.S. Government and is not subject to copyright protection in the United States.

*Aerospace Engineer, Code VN5T, 5280 Fourth Street; schumach@nsc.navy.mil. Senior Member AIAA.
†Engineering Scientist, Code 7215, 4555 Overlook Avenue, SE.
‡Project Engineer, 7515 Mission Drive.
§Physicist, 5280 Fourth Street.

η_D = quantum efficiency of laser-ranging detector
η_R = SLR receiver efficiency
η_T = SLR transmitter efficiency
θ_T = SLR beam divergence half-angle
θ_T^* = gain-optimum SLR beam divergence half-angle
λ = longitude of surveillance station
λ_0 = wavelength of laser
ρ_c = slant range between calibration station and satellite
ρ_s = slant range between surveillance station and satellite
σ = laser target apparent cross-sectional area
ϕ = geodetic latitude of surveillance station
ψ = azimuth of satellite at calibration station

I. Introduction

SURVEILLANCE of space by the Naval Space Surveillance System, commonly known as the Fence, and by two dozen other U.S. Army and U.S. Air Force tracking systems is the primary way United States Space Command maintains comprehensive space situational awareness. The Fence is unique in the inventory of surveillance assets and contributes a large share of the observational base for the catalog of trackable space objects. About 80% of all known space objects eventually make detectable passes through its field of view, including 87% of all satellites having orbital periods below 1100 min.

In essence, the Fence is a multistatic continuous-waveradar interferometer consisting of three transmitters and six receivers deployed on a great-circle arc across the southern United States. The station beam patterns overlap in such a way that all detections and measurements are made close to the nominal great-circle plane, which is inclined at 33 deg to the equator. Some details about the system can be found in Ref. 1. The Fence system as a whole detects about 22,000 satellite passes daily, a number determined mainly by the orbital kinematics of the current population of about 9500 trackable space objects. On average, each pass through the Fence plane is illuminated by two transmitters and detected by four receivers. The result is that more than 160,000 satellite detections are recorded daily. For each detection raw signal phase and amplitude measurements from each receiver are processed by means of interferometric algorithms into a pair of direction cosines giving the apparent angular position of the target. The detections are made, and the direction cosines are produced without any a priori knowledge of the satellite population. Subsequently, the cosines are associated with known space objects in real time.

Traditionally, the Fence data quality has been assessed in terms of statistics on cosine residuals computed with Brouwer-type mean elements for the cataloged orbits. By this measure, the nominal cosine precision is about 0.0002 in rms sense. Additionally, internal phase calibration of the antenna and detector electronics, applied every 30 min, provides a measure of the apparent noise floor of the metric data. This value is approximately 0.00001 rms in units of direction cosine (10 μrad on a zenith pass) and is believed to be almost constant over time.

The difficulty with these statistics is that they do not provide a true assessment of Fence metric performance. The cataloged mean elements are derived from general perturbation orbit models whose known errors are larger than the expected random measurement errors in the Fence system. Moreover, the rms statistic does not distinguish systematic from random errors. The internal calibration does compensate for some systematic effects as a result of localized environmental and physical changes in the antenna and receiver systems, but cannot provide any measure of absolute system accuracy. Previous results with Fence data show that surveillance data calibration, together with orbit model improvements, does permit more accurate orbit solutions for the space catalog.[2] However, a true assessment of Fence accuracy and precision can be obtained on a practical basis using satellite laser ranging (SLR). The present work describes how precisely Fence data can be calibrated using SLR techniques.

II. Two SLR-Based Calibration Methods

Two different methods of calibrating Fence data have been investigated. The advantages and limitations of each have been discussed in Ref. 3 in terms of precision and space surveillance operational needs and are summarized here.

A. Ephemeris Method

The public availability of globally distributed, SLR data for scientific payloads at different altitudes makes possible the continuous production of high-precision reference ephemerides for these satellites. For example, geodetic work sometimes requires satellite positions to be estimated a posteriori to within several centimeters in an Earth-fixed frame. However, any ephemerides with position errors of as large as 10 m are potentially useful for calibrating present-day space surveillance measurements, as long as they can be interpolated to the times of the surveillance observations of those objects. Use of postfit ephemerides of SLR-tracked satellites for Fence data calibration is now being implemented for surveillance operations because of the reliability with which continuous, high-precision reference orbits can be produced. One disadvantage of the postfit ephemeris method is that there is a latency of about three days in the reference data. Given the present-day capacity of SLR tracking systems, this lag is necessary if known and nearly uniform ephemeris quality is to be maintained for reference satellites over a wide range of altitudes. Real-time calibration would be possible if prediction ephemerides were used. However, prediction ephemerides are not now being proposed for operational Fence data calibration because the calibration precision would be poorly known.

B. Simultaneous-Track Method

An alternative to using prediction ephemerides for calibration is to make SLR measurements of a target simultaneously with the surveillance measurements and comparing these data directly. The proximity of an SLR site to a Fence receiver means that satellites will often be in common view of both stations. If a sufficiently precise three-dimensional position of a satellite can be computed directly from SLR ranges and measured telescope angles as it crosses the Fence, then a near real-time comparison of Fence data with simultaneous SLR data can be made without the complexities of high-precision orbit determination. This type of comparison might serve as an occasional spot-check calibration and could aid in making certain equipment adjustments at the Fence stations. A key question, which has been raised in previous work,[1] is whether co-locating the SLR station with a Fence station benefits this type of calibration. Also, the practicality of simultaneous-track calibration depends on at least two other factors:

1) Tasking: SLR operations are sensitive to weather, which can affect yield over a site. Additionally, existing SLR facilities often have competing missions to accomplish.

2) Precision of SLR and telescope-derived position: With most SLR systems, because of beam divergence coupled with boresight pointing errors, the position uncertainty is almost entirely caused by uncertainty in the SLR measured angles.

III. Precision of Ephemeris Method

Each Fence receiver station contributes a pair of direction cosines reckoned in the local horizontal plane as defined next. The geometrical relation between satellite position $\boldsymbol{r} = (x, y, z)^T$ and Fence direction cosines measured at the same time at one of the Fence receiver stations is

$$\boldsymbol{r} = \boldsymbol{R}_s + \boldsymbol{u}_s \rho_s \tag{1}$$

where ρ_s is the slant range between the Fence station and the satellite (Fig. 1). It is assumed that light-time correction has been taken into account in obtaining the satellite position from the ephemeris: given a Fence observation reckoned at time t, the corresponding ephemeris time is $t - \rho_s/c$. The local topocentric frame at the Fence station is defined by an orthonormal vector basis $(\boldsymbol{H}_s, \boldsymbol{E}_s, \boldsymbol{N}_s)$, representing the local geodetic vertical (positive up), local east, and local north directions, respectively. An azimuth rotation around the local vertical through angle A, positive east of north, defines the Fence local frame $(\boldsymbol{H}'_s, \boldsymbol{E}'_s, \boldsymbol{N}'_s)$ in which the direction cosines are reckoned:

$$\boldsymbol{H}'_s = \boldsymbol{H}_s, \qquad \boldsymbol{E}'_s = \boldsymbol{E}_s \cos A - \boldsymbol{N}_s \sin A$$

$$\boldsymbol{N}'_s = \boldsymbol{E}_s \sin A + \boldsymbol{N}_s \cos A \tag{2}$$

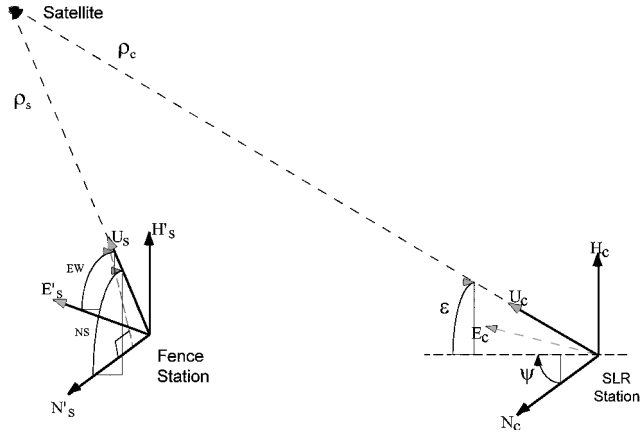

Fig. 1 Sighting geometry for simultaneous-track calibration.

Then

$$\boldsymbol{u}_s = \sqrt{1-m^2-n^2}\,\boldsymbol{H}'_s + m\boldsymbol{E}'_s + n\boldsymbol{N}'_s \tag{3}$$

where m and n are the nominal Fence observables. From Eq. (1) the line-of-sight unit vector is equal to

$$\boldsymbol{u}_s = (1/\rho_s)(\boldsymbol{r}-\boldsymbol{R}_s) \tag{4}$$

so that the components of interest are

$$m = (1/\rho_s)\boldsymbol{E}'^T_s(\boldsymbol{r}-\boldsymbol{R}_s), \qquad n = (1/\rho_s)\boldsymbol{N}'^T_s(\boldsymbol{r}-\boldsymbol{R}_s) \tag{5}$$

Now consider variations of m and n with respect to variations in ephemeris position and station position. Conceptually, $m = f(x, y, z, X_s, Y_s, Z_s)$ so that

$$\delta m = \frac{\partial f}{\partial x}\delta x + \frac{\partial f}{\partial y}\delta y + \frac{\partial f}{\partial z}\delta z + \frac{\partial f}{\partial X_s}\delta X_s + \frac{\partial f}{\partial Y_s}\delta Y_s + \frac{\partial f}{\partial Z_s}\delta Z_s \tag{6}$$

For an approximate error analysis assume that all variations on the right-hand side are uncorrelated so that their net effect is described by a quadratic sum[4,5]:

$$(\delta m)^2 = \left(\frac{\partial f}{\partial x}\right)^2(\delta x)^2 + \left(\frac{\partial f}{\partial y}\right)^2(\delta y)^2 + \left(\frac{\partial f}{\partial z}\right)^2(\delta z)^2 + \left(\frac{\partial f}{\partial X_s}\right)^2(\delta X_s)^2 + \left(\frac{\partial f}{\partial Y_s}\right)^2(\delta Y_s)^2 + \left(\frac{\partial f}{\partial Z_s}\right)^2(\delta Z_s)^2 \tag{7}$$

There is some freedom in how the variations in this linearized error description are interpreted. For example, each squared variation can be taken as the variance (squared standard deviation) of the quantity, when it is convenient to do so. For now, this expression can be simplified by assigning the same nominal value to each component of ephemeris error, and likewise for each component of station location error:

$$\delta x = \delta y = \delta z = \delta E, \qquad \delta X_s = \delta Y_s = \delta Z_s = \delta S \tag{8}$$

so that Eq. (7) can be written as

$$(\delta m)^2 = \frac{\partial f}{\partial \boldsymbol{r}}\left(\frac{\partial f}{\partial \boldsymbol{r}}\right)^T(\delta E)^2 + \frac{\partial f}{\partial \boldsymbol{R}_s}\left(\frac{\partial f}{\partial \boldsymbol{R}_s}\right)^T(\delta S)^2 \tag{9}$$

Given nominal errors in the ephemeris and station location, this formula gives the corresponding error in east–west direction cosine. This cosine error is the smallest that can be resolved by comparisons with the reference ephemeris. In practice, correlations always exist among the components of position error, and so some contributions to the cosine error magnitude are omitted from Eq. (7). However, the nominal position errors in Eq. (9) can be chosen to try to make up for that omission. In many real cases the correlation terms missing from a general error formula like Eq. (7) are not well known so that one has to make some conservative assumptions about the nominal errors in order to arrive at useful results.

Although the concept is simple, obtaining explicit expressions for the gradients and their inner products involves some algebraic manipulation. The steps are as follows. The functional form of m is given by Eq. (5) as $f = g(\boldsymbol{r}, \boldsymbol{R}_s, \rho_s, \boldsymbol{E}'_s)$; therefore, the chain rule is used:

$$\frac{\partial f}{\partial \boldsymbol{r}} = \frac{\partial g}{\partial \boldsymbol{r}} + \frac{\partial g}{\partial \rho_s}\frac{\partial \rho_s}{\partial \boldsymbol{r}} = \frac{1}{\rho_s}\boldsymbol{E}'^T_s + \left[-\frac{1}{\rho_s^2}\boldsymbol{E}'^T_s(\boldsymbol{r}-\boldsymbol{R}_s)\right]\frac{\partial \rho_s}{\partial \boldsymbol{r}} = \frac{1}{\rho_s}\boldsymbol{E}'^T_s - \frac{m}{\rho_s}\frac{\partial \rho_s}{\partial \boldsymbol{r}} \tag{10}$$

Squaring Eq. (1), obtain $\rho_s^2 = (\boldsymbol{r}-\boldsymbol{R}_s)^T(\boldsymbol{r}-\boldsymbol{R}_s)$, and by differentiation

$$\frac{\partial \rho_s}{\partial \boldsymbol{r}} = \frac{1}{\rho_s}(\boldsymbol{r}-\boldsymbol{R}_s)^T \tag{11}$$

Then Eq. (10) becomes

$$\frac{\partial f}{\partial \boldsymbol{r}} = \frac{1}{\rho_s}\boldsymbol{E}'^T_s - \frac{1}{\rho_s^2}m(\boldsymbol{r}-\boldsymbol{R}_s)^T \tag{12}$$

and the coefficient of nominal ephemeris error is

$$\frac{\partial f}{\partial \boldsymbol{r}}\left(\frac{\partial f}{\partial \boldsymbol{r}}\right)^T = \frac{1}{\rho_s^2}(1-m^2) \tag{13}$$

The gradient with respect to Fence station position is more complicated. The chain rule is

$$\frac{\partial f}{\partial \boldsymbol{R}_s} = \frac{\partial g}{\partial \boldsymbol{R}_s} + \frac{\partial g}{\partial \rho_s}\frac{\partial \rho_s}{\partial \boldsymbol{R}_s} + \frac{\partial g}{\partial \boldsymbol{E}'_s}\frac{\partial \boldsymbol{E}'_s}{\partial \boldsymbol{R}_s} \tag{14}$$

so that

$$\frac{\partial f}{\partial \boldsymbol{R}_s} = -\frac{1}{\rho_s}\boldsymbol{E}'^T_s + \frac{1}{\rho_s^2}m(\boldsymbol{r}-\boldsymbol{R}_s)^T + \frac{1}{\rho_s}(\boldsymbol{r}-\boldsymbol{R}_s)^T\frac{\partial \boldsymbol{E}'_s}{\partial \boldsymbol{R}_s} \tag{15}$$

Most of the complication occurs in the latter partial derivative (Jacobian matrix). The Fence local east unit vector depends on the local topocentric basis vectors, as shown in Eq. (2). The local topocentric basis vectors are functions of station position via the definitions

$$\begin{aligned}\boldsymbol{H}_s &= (\cos\varphi\cos\lambda, \cos\varphi\sin\lambda, \sin\varphi)^T\\ \boldsymbol{E}_s &= (-\sin\lambda, \cos\lambda, 0)^T\\ \boldsymbol{N}_s &= (-\sin\varphi\cos\lambda, -\sin\varphi\sin\lambda, \cos\varphi)^T\end{aligned} \tag{16}$$

where φ is the geodetic latitude. If the squared eccentricity of the geodetic reference ellipsoid is neglected compared to unity, a relative error of less than 1% is introduced in the last term of Eq. (15), namely, $e^2 = 0.006694$, approximately.[6] This approximation allows the local topocentric basis vectors to be expressed in simple explicit terms of station position:

$$\boldsymbol{H}_s = \|\boldsymbol{R}_s\|^{-1}\boldsymbol{R}_s, \qquad \boldsymbol{E}_s = \|\boldsymbol{k}\times\boldsymbol{H}_s\|^{-1}\boldsymbol{k}\times\boldsymbol{H}_s, \qquad \boldsymbol{N}_s = \boldsymbol{H}_s\times\boldsymbol{E}_s \tag{17}$$

where $\boldsymbol{k}$ constant in an Earth-fixed frame. The chain rule is now straightforward though lengthy. The final result, the coefficient of nominal station position error in Eq. (9), is

$$\frac{\partial f}{\partial \boldsymbol{R}_s}\left(\frac{\partial f}{\partial \boldsymbol{R}_s}\right)^T = \frac{1}{\rho_s^2}(1-m^2) + \frac{2(1-m^2)\sqrt{1-m^2-n^2}}{\rho_s R_s} + \frac{1-m^2-n^2}{R_s^2} + \frac{n\sin\varphi}{\rho_s R_s \cos\varphi}\Big[-2\cos A + 2m(m\cos A + n\sin A) + \frac{\rho_s}{R_s\cos\varphi}\left(n\sin\varphi - 2\cos\varphi\cos A\sqrt{1-m^2-n^2}\right)\Big] \tag{18}$$

where $R_s = \|\boldsymbol{R}_s\|$.

The special case of zenith pass over a Fence station ($m = n = 0$) is instructive because Eqs. (13) and (18) reduce to simple forms:

$$\frac{\partial f}{\partial \boldsymbol{r}}\left(\frac{\partial f}{\partial \boldsymbol{r}}\right)^T = \frac{1}{\rho_s^2}, \qquad \frac{\partial f}{\partial \boldsymbol{R}_s}\left(\frac{\partial f}{\partial \boldsymbol{R}_s}\right)^T = \left(\frac{1}{\rho_s} + \frac{1}{R_s}\right)^2 \tag{19}$$

Moreover, inspection of the full expressions (13) and (18) shows that the first three terms of Eq. (18), which are always positive, take their maximum values on a zenith pass. The remaining terms have a factor that is proportional to one of the cosines, and so the terms will be sometimes positive and sometimes negative, depending on the pass geometry. Hence, for a set of many passes, randomly selected, the zenith passes will tend to be the worst case for the ephemeris-method calibration precision. This fact makes the simple zenith-pass formulas useful for quickly estimating calibration requirements. The "worst of the worst" cases will be, on average, low-altitude zenith passes over a station ($\rho_s \ll R_s$), for which the ephemeris uncertainty and the station location uncertainty affect the resolvable east–west cosine error in almost the same way.

Some representative numerical results for the zenith case are summarized in Table 1. Nominal satellite altitudes have been used for four real calibration candidates, slant ranges have been set equal to altitude, and station position magnitudes have been set equal to the Earth equatorial radius of 6,378,137.0 m. A nominal station location uncertainty of 2 m has been assigned as representative of survey precision for existing Fence stations. Nominal ephemeris uncertainties have been taken from previous work.[3] These ephemeris uncertainties are typical of "quick-look" three-day fit precisions that are expected in reference data for Fence calibration. For all four example satellites the level of cosine error estimated to be resolvable by the ephemeris method is well below the current system noise floor of 10-μrad standard deviation at zenith.

The analysis for north–south direction cosine proceeds in exactly the same way. An error relation analogous to Eq. (9) is developed, using the functional form of n given in Eq. (5):

$$(\delta n)^2 = \frac{\partial f'}{\partial \boldsymbol{r}}\left(\frac{\partial f'}{\partial \boldsymbol{r}}\right)^T (\delta E)^2 + \frac{\partial f'}{\partial \boldsymbol{R}_s}\left(\frac{\partial f'}{\partial \boldsymbol{R}_s}\right)^T (\delta S)^2 \tag{20}$$

The coefficients turn out to be

$$\frac{\partial f'}{\partial \boldsymbol{r}}\left(\frac{\partial f'}{\partial \boldsymbol{r}}\right)^T = \frac{1}{\rho_s^2}(1-n^2) \tag{21}$$

and

$$\frac{\partial f'}{\partial \boldsymbol{R}_s}\left(\frac{\partial f'}{\partial \boldsymbol{R}_s}\right)^T = \frac{1}{\rho_s^2}(1-n^2) + \frac{2(1-n^2)\sqrt{1-m^2-n^2}}{\rho_s R_s} + \frac{1-m^2-n^2}{R_s^2} + \frac{m\sin\varphi}{\rho_s R_s\cos\varphi}\Big[+2\sin A - 2n(m\cos A + n\sin A) + \frac{\rho_s}{R_s\cos\varphi}\left(m\sin\varphi + 2\cos\varphi\sin A\sqrt{1-m^2-n^2}\right)\Big] \tag{22}$$

These formulas reduce to the same form as Eq. (19) for a zenith pass, and otherwise have the same properties just mentioned.

IV. Precision of Simultaneous-Track Method

The basic geometrical relation between Fence direction cosines and simultaneous SLR measurements is

$$\boldsymbol{R}_c + \boldsymbol{u}_c\rho_c = \boldsymbol{R}_s + \boldsymbol{u}_s\rho_s \tag{23}$$

In terms of local topocentric basis vectors, as shown in Fig. 1, the SLR line of sight is given by

$$\boldsymbol{u}_c = \boldsymbol{H}_c\sin\varepsilon + \boldsymbol{E}_c\cos\varepsilon\sin\psi + \boldsymbol{N}_c\cos\varepsilon\cos\psi \tag{24}$$

Solving Eq. (23) for the Fence measured line-of-sight unit vector, obtain

$$\boldsymbol{u}_s = (\rho_c/\rho_s)\boldsymbol{u}_c + (1/\rho_s)(\boldsymbol{R}_c - \boldsymbol{R}_s) \tag{25}$$

so that the components of interest are

$$m = (\rho_c/\rho_s)\left[\left(\boldsymbol{E}_s'^T\boldsymbol{H}_c\right)\sin\varepsilon + \left(\boldsymbol{E}_s'^T\boldsymbol{E}_c\right)\cos\varepsilon\sin\psi + \left(\boldsymbol{E}_s'^T\boldsymbol{N}_c\right)\cos\varepsilon\cos\psi\right] + (1/\rho_s)\boldsymbol{E}_s'^T(\boldsymbol{R}_c - \boldsymbol{R}_s) \tag{26}$$

$$n = (\rho_c/\rho_s)\left[\left(\boldsymbol{N}_s'^T\boldsymbol{H}_c\right)\sin\varepsilon + \left(\boldsymbol{N}_s'^T\boldsymbol{E}_c\right)\cos\varepsilon\sin\psi + \left(\boldsymbol{N}_s'^T\boldsymbol{N}_c\right)\cos\varepsilon\cos\psi\right] + (1/\rho_s)\boldsymbol{N}_s'^T(\boldsymbol{R}_c - \boldsymbol{R}_s) \tag{27}$$

These expressions give the direction cosines in the functional form $m = f(\boldsymbol{u}_c, \boldsymbol{E}_s', \rho_c, \rho_s, \boldsymbol{R}_c, \boldsymbol{R}_s)$. Considering variations of the direction cosines with respect to variations in SLR measurements and station locations, one needs the chain rules

$$\frac{\partial m}{\partial \rho_c} = \frac{\partial f}{\partial \rho_c}, \qquad \frac{\partial m}{\partial \varepsilon} = \frac{\partial f}{\partial \boldsymbol{u}_c}\frac{\partial \boldsymbol{u}_c}{\partial \varepsilon}, \qquad \frac{\partial m}{\partial \psi} = \frac{\partial f}{\partial \boldsymbol{u}_c}\frac{\partial \boldsymbol{u}_c}{\partial \psi} \tag{28}$$

$$\frac{\partial m}{\partial \boldsymbol{R}_s} = \frac{\partial f}{\partial \boldsymbol{R}_s} + \frac{\partial f}{\partial \rho_s}\frac{\partial \rho_s}{\partial \boldsymbol{R}_s} + \frac{\partial f}{\partial \boldsymbol{E}_s'}\frac{\partial \boldsymbol{E}_s'}{\partial \boldsymbol{R}_s}$$

$$\frac{\partial m}{\partial \boldsymbol{R}_c} = \frac{\partial f}{\partial \boldsymbol{R}_c} + \frac{\partial f}{\partial \rho_c}\frac{\partial \rho_c}{\partial \boldsymbol{R}_c} + \frac{\partial f}{\partial \boldsymbol{u}_c}\frac{\partial \boldsymbol{u}_c}{\partial \boldsymbol{R}_s} \tag{29}$$

The variations with respect to station positions are lengthy expressions, as before. However, the variations with respect to SLR measurements are easy to derive. Moreover, the relative uncertainties in measured angle are expected to be much larger than the relative uncertainties in measured range for SLR systems. Therefore, for a first investigation of the errors in the simultaneous-track method, consider only angle variations.

Table 1 Cosine precisions resolvable by ephemeris method (zenith pass)

Satellite	ERS-2	TOPEX	LAGEOS	GPS-35
Altitude, km	782	1340	5861	20,135
Ephemeris position uncertainty, m	1.47	0.69	0.22	5.96
Ephemeris coefficient, 1/m^2	164×10^{-14}	56×10^{-14}	3×10^{-14}	0.2×10^{-14}
Station position uncertainty, m	2	2	2	2
Station coefficient, 1/m^2	206×10^{-14}	82×10^{-14}	11×10^{-14}	4×10^{-14}
Cosine uncertainty, μrad at zenith	3.4	1.9	0.7	0.4

From Eqs. (26) and (27) obtain

$$\delta m = (\rho_c/\rho_s)\left[\left(\boldsymbol{E}_s'^T\boldsymbol{H}_c\right)\cos\varepsilon - \left(\boldsymbol{E}_s'^T\boldsymbol{E}_c\right)\sin\varepsilon\sin\psi - \left(\boldsymbol{E}_s'^T\boldsymbol{N}_c\right)\sin\varepsilon\cos\psi\right]\delta\varepsilon + (\rho_c/\rho_s)\left[\left(\boldsymbol{E}_s'^T\boldsymbol{E}_c\right)\cos\psi - \left(\boldsymbol{E}_s'^T\boldsymbol{N}_c\right)\sin\psi\right]\delta\psi\cos\varepsilon \quad (30)$$

$$\delta n = (\rho_c/\rho_s)\left[\left(\boldsymbol{N}_s'^T\boldsymbol{H}_c\right)\cos\varepsilon - \left(\boldsymbol{N}_s'^T\boldsymbol{E}_c\right)\sin\varepsilon\sin\psi - \left(\boldsymbol{N}_s'^T\boldsymbol{N}_c\right)\sin\varepsilon\cos\psi\right]\delta\varepsilon + (\rho_c/\rho_s)\left[\left(\boldsymbol{N}_s'^T\boldsymbol{E}_c\right)\cos\psi - \left(\boldsymbol{N}_s'^T\boldsymbol{N}_c\right)\sin\psi\right]\delta\psi\cos\varepsilon \quad (31)$$

It would be straightforward to rewrite these expressions as quadratic sums, giving two explicit error relations under the assumption that all of the errors are uncorrelated. However, it proves to be convenient to invert these equations to give the SLR angle variations in terms of the direction cosine variations. The equations have the form

$$\frac{\rho_c}{\rho_s}\begin{bmatrix} a_{11} & a_{12} \\ a_{21} & a_{22}\end{bmatrix}\begin{Bmatrix}\delta\varepsilon \\ \delta\psi\cos\varepsilon\end{Bmatrix} = \begin{Bmatrix}\delta m \\ \delta n\end{Bmatrix} \quad (32)$$

where the coefficients are defined by correspondence with Eqs. (30) and (31). Then

$$\begin{Bmatrix}\delta\varepsilon \\ \delta\psi\cos\varepsilon\end{Bmatrix} = \frac{1}{\Delta}\frac{\rho_s}{\rho_c}\begin{bmatrix} a_{22} & -a_{12} \\ -a_{21} & a_{11}\end{bmatrix}\begin{Bmatrix}\delta m \\ \delta n\end{Bmatrix}$$

where

$$\Delta = a_{11}a_{22} - a_{12}a_{21} \quad (33)$$

Rewrite this pair of equations as quadratic sums:

$$(\delta\varepsilon)^2 = (1/\Delta^2)\left(\rho_s^2/\rho_c^2\right)\left[a_{22}^2(\delta m)^2 + a_{12}^2(\delta n)^2\right] \quad (34)$$

$$(\delta\psi)^2\cos^2\varepsilon = (1/\Delta^2)\left(\rho_s^2/\rho_c^2\right)\left[a_{21}^2(\delta m)^2 + a_{11}^2(\delta n)^2\right] \quad (35)$$

Now define the SLR total angular measurement error $\delta\Theta$ by adding these two component errors. Also, it is convenient to assign the same nominal value to both direction cosine error components: $\delta m = \delta n = \delta\beta$. Then

$$(\delta\Theta)^2 = (\delta\varepsilon)^2 + (\delta\psi)^2\cos^2\varepsilon = \frac{\rho_s^2\left(a_{11}^2 + a_{12}^2 + a_{21}^2 + a_{22}^2\right)}{\rho_c^2(a_{11}a_{22} - a_{12}a_{21})^2}(\delta\beta)^2 = K\,(\delta\beta)^2 \quad (36)$$

Here the factors a_{ij} are given by Eqs. (30–32), and the necessary unit vectors are given by their definitions (2) and (16), as needed for each station. If the squared eccentricity of the geodetic reference ellipsoid is neglected compared to unity as before, then the form of Eq. (17) applies for the topocentric basis vectors at each station.

Equation (36) gives the SLR angular measurement precision that is equivalent to a given direction cosine precision on a given satellite pass. It approximates the largest SLR angular precision that can be used to calibrate the direction cosines to a given nominal precision, or the direction cosine error level that can be resolved with a given SLR facility. The relation implies that large values of K are desirable for calibration by the simultaneous-track method, if there are no other considerations. The reason is that the resolvable cosine precision is less sensitive to SLR angular measurement precision, in that case.

The coefficient K is ultimately a function of Fence station position, SLR station position and satellite position so that it is strongly dependent on sighting geometry. The functional dependence on these positions is too complicated to allow easy analytical characterization. However, it is worth noting that if the Fence station and the SLR station are exactly co-located, then the coefficient K reduces to a simple function of elevation angle:

$$(\delta\Theta)^2 = (\delta\varepsilon)^2 + (\delta\psi)^2\cos^2\varepsilon = \frac{1+\sin^2\varepsilon}{\sin^2\varepsilon}(\delta\beta)^2 \quad (37)$$

This can be proven straightforwardly from the preceding equations, and the result is intuitively plausible. It says that, for given cosine precision, the requirement on angular measurement precision is most stringent at zenith and least stringent near the horizon. In other words, the best cosine calibration precision is obtained at the lowest usable elevation, if there are no other considerations such as the deleterious effects of the atmosphere.

Figures 2–5 show K as a function of longitude, elevation as seen from the Fence receiver site, or calibrator latitude. These graphs are essentially engineering tools, which give insight into the extent to which the laser divergence and system pointing accuracy must be refined for a given calibrator and fence sensor location.

Figure 2 shows values of K plotted vs longitude for some real satellite passes used in previous work.[1] In these cases the SLR station was the Naval Research Laboratory's system integrated on the 3.5-m telescope at Starfire Optical Range (NRL@SOR) at Kirtland Air Force Base, New Mexico, longitude approximately 254° (Ref. 7). This site is only about 150 km north of the Elephant Butte receiver station, so that most Fence passes visible at Elephant Butte were also visible at NRL@SOR.

The figure indicates that the value of the factor K is indeed highly pass dependent. The implication is that simultaneous-track

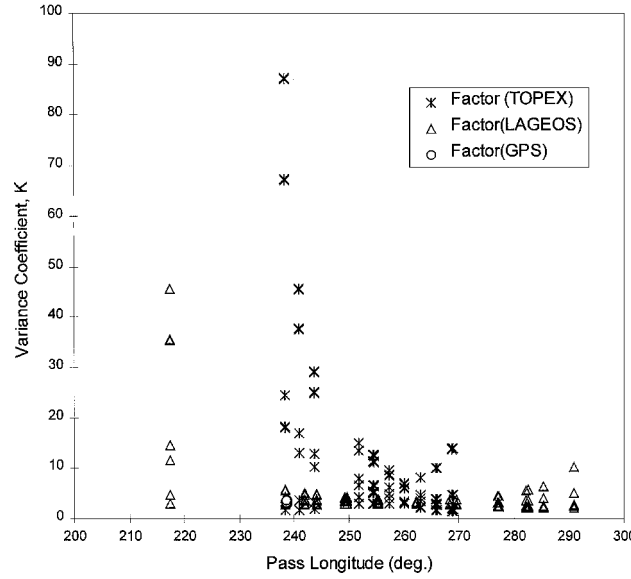

Fig. 2 Variance coefficient K vs pass longitude (real data).

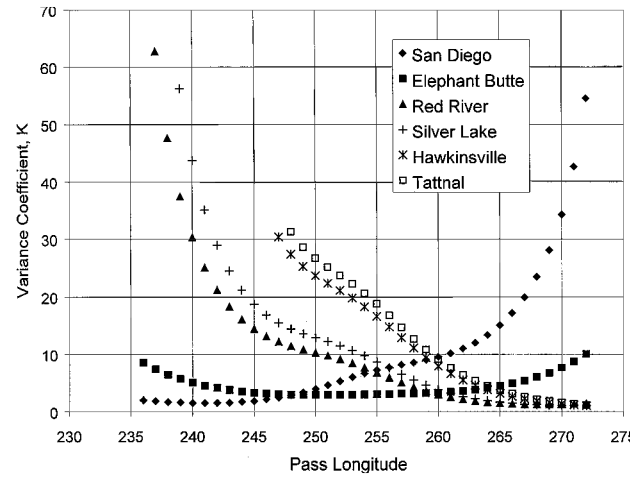

Fig. 3 Variance coefficient K vs pass longitude (simulated data).

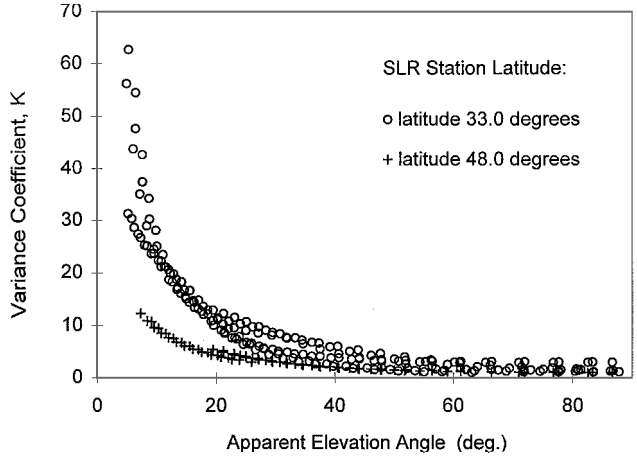

Fig. 4 Variance coefficient K vs apparent elevation angle as seen from Fence receivers (simulated data).

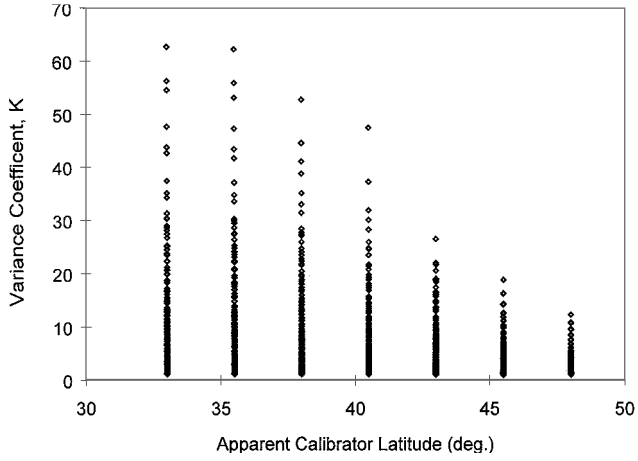

Fig. 5 Variance coefficient K vs apparent elevation angle for various calibrator latitudes as seen from Fence receivers (simulated data).

calibration has to be carefully planned and suitable passes selected well in advance of the data collection. Sufficiently large values of K may occur infrequently for given station locations and given target satellites. In particular, NRL@SOR used a beam divergence half-angle of 50 μrad. The host telescope had a nominal boresight pointing uncertainty at least an order of magnitude smaller than this, about one arcsecond, so that the SLR angular measurement uncertainty was almost entirely caused by beam divergence. Equation (36) indicates that if Fence cosines were to be calibrated to the assumed noise floor of 10^{-5} using these passes, then the factor K would have to be at least 25. Of the real passes shown in Fig. 2, most did not meet this criterion. However, usable passes occurred often enough that they could have been considered as "targets of opportunity" to support calibration adjustments of Fence field station equipment.

Figure 3 shows values of K plotted vs longitude of Fence crossing for a simulated pass of a hypothetical target detected in the Fence plane at an altitude of 1000 km. The NRL@SOR coordinates were used for the SLR calibrator. The sensor locations were the six Fence receivers, which are named in the legend of the figure. Assuming a beam divergence half-angle of 50 μrad, the proportion of usable passes ($K \geq 25$) turns out to be approximately the same as for the small sample of real passes shown in Fig. 2. Also, as with the real dataset, it is clear that many more passes would become usable for simultaneous-track calibration if a smaller beam divergence were used.

Other features of the simulated pass data are shown in Figs. 4 and 5. Figure 4 plots values of K vs elevation angle seen at Fence receivers, which has been labeled "apparent elevation angle." The trend is for usable passes to occur at low Fence elevations. In fact, the largest values of K usually do occur when the target is close to the SLR site and far from the Fence receiver site, a consequence of the way the two ranges enter into Eq. (36). Because both stations are on the surface of the Earth, the Fence station necessarily sees the target at low elevation angles. In practice, Fence measurements are made down to about 5-deg elevation, and most of the simulated passes with $K \geq 25$ occurred near this lower limit. In this plot the advantage of using a smaller beam divergence is apparent because many more passes would become candidates for simultaneous-track calibration.

Figure 5 shows the effect of moving the SLR station to different sites relative to the Fence stations. In this case the simulated SLR station always had the same longitude as NRL@SOR but was placed at different latitudes north of the nominal Fence latitude of 33°. The simulation shows that there is some advantage in having the SLR site near the Fence plane if simultaneous-track calibration is to be done. The extent of the advantage for real target satellites would have to be examined on a case-by-case basis because real target passes through the Fence are not distributed uniformly in longitude. These results indicate that it is co-location with respect to the Fence plane rather than to the receivers themselves that provides more opportunities for sufficiently precise calibration.

V. SLR Angular Measurement Error

The analysis for simultaneous-track calibration raises the general question of how precisely SLR systems can measure angular position and therefore position in space. This question requires some comment because most SLR applications are based solely on precise range measurements, without regard for observing three-dimensional position directly. Typically, the angular tracking precision has to be sufficient merely to guarantee that enough photoelectrons will be available in the SLR receiver for a detection to be made. The number of photoelectrons available N_{pe} is given by the link equation[8]:

$$N_{\text{pe}} = \eta_D E_0 (\lambda_0/hc) \eta_T G_T \sigma \left(1/4\pi\rho_c^2\right)^2 A_R \eta_R T_a^2 T_c^2 \tag{38}$$

For a beam with a Gaussian intensity profile, the transmitter gain depends on two other factors:

$$G_T = \left(8/\theta_T^2\right) \exp\left[-2\left\{(\delta\theta)^2/\theta_T^2\right\}\right] \tag{39}$$

The quantity $\delta\theta$ is the nominal pointing uncertainty, resulting from mechanically induced random variations (jitter) in the boresight direction. The quantity θ_T is the beam divergence half-angle.

The form of the gain equation indicates that, for a given pointing uncertainty, there is some value of the beam divergence that maximizes the transmitter gain. The optimum beam divergence can be found from the necessary condition:

$$\frac{\mathrm{d}G_T}{\mathrm{d}\theta_T} = 0 \tag{40}$$

The algebra is simplified if the intermediate variable $p = 1/\theta_T^2$ is defined so that Eq. (39) becomes

$$G_T = 8p \exp[-2(\delta\theta)^2 p] \tag{41}$$

Then the derivative is computed as

$$\frac{\mathrm{d}G_T}{\mathrm{d}\theta_T} = \frac{\mathrm{d}G_T}{\mathrm{d}p}\frac{dp}{\mathrm{d}\theta_T} = \{8\exp[-2(\delta\theta)^2 p]$$

$$-16p(\delta\theta)^2 \exp[-2(\delta\theta)^2 p]\}\left(-\frac{2}{\theta_T^3}\right) = 0 \tag{42}$$

$$8\exp[-2(\delta\theta)^2 p][1 - 2p(\delta\theta)^2]\left(-\frac{2}{\theta_T^3}\right) = 0 \tag{43}$$

For finite beam divergence angles only the middle factor can vanish. Therefore, the gain-optimum value of beam divergence half-angle is

$$\theta_T^* = \sqrt{2}\,\delta\theta \tag{44}$$

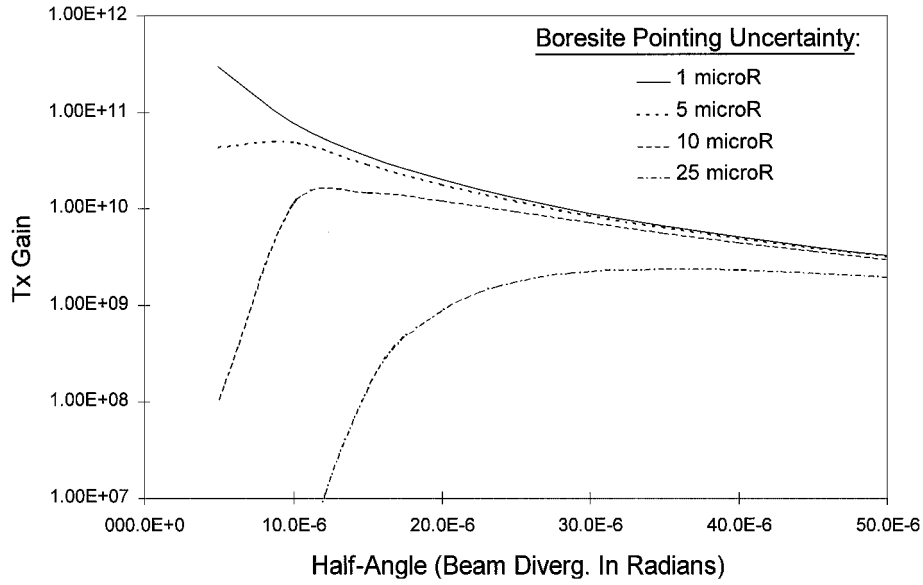

Fig. 6 SLR transmitter gain vs beam divergence half-angle for various boresight pointing errors.

and the optimum gain is

$$G_T^* = 8/2e(\delta\theta)^2 = 8/e\left(\theta_T^*\right)^2 \tag{45}$$

where e is the base of natural logarithms.

If the objective of the laser tracking is to guarantee detection and measure precise ranges, there is little reason to use a beam divergence of less than the optimum value. However, if the objective were to measure position directly, then one would like to have the smallest beam divergence that still produces a usable gain. The reason is that the angular measurement precision depends on both the pointing uncertainty and the beam divergence:

$$(\delta\Theta)^2 = (\delta\varepsilon)^2 + (\delta\psi)^2\cos^2\varepsilon = (\delta\theta)^2 + \theta_T^2 \tag{46}$$

This relation expresses the fact that, even with perfect pointing, one still does not know where in the beam the detection is made. At the gain-optimum value of beam divergence, the total angular measurement variance is three times the boresight pointing variance. For beam divergences above the gain-optimum value, one can improve both the gain and the total angular measurement variance by reducing the divergence. Below the gain-optimum value, reducing the beam divergence involves a tradeoff between gain and angular measurement variance. This tradeoff is illustrated for typical SLR systems in Fig. 6. For beam divergences below the gain-optimum value, reducing the beam divergence also reduces the gain, making the likelihood of detection smaller. The decreased probability of detection is the main reason why SLR tracking with very small beam divergences is difficult to accomplish in practice. Moreover, with very small beam divergences other operational problems can arise. In particular, the energy density of the beam might exceed a threshold for interference or damage to systems on the target satellite or even on other satellites that inadvertently cross the beam. In the latter case laser clearinghouse restrictions would constrain the times and directions for which narrow-beam illumination could be attempted.

Finally, it may be remarked that the boresight pointing variance is typically difficult to measure in real time. However, if the beam divergence could be changed accurately during a pass, then in principle it would be possible to estimate an effective value of the pointing variance (e.g., including atmospheric effects) by simple photon counting. Suppose the number of photoelectrons is measured at two different points in the pass using two different values of the transmitter gain. The link equation (38) evaluated at each point results in the ratio

$$N_{\mathrm{pe}1}/N_{\mathrm{pe}2} = (G_{T1}/G_{T2})\left(\rho_{c2}^4/\rho_{c1}^4\right) \tag{47}$$

assuming that all of the other factors are the same at both points. The ratio of gains is

$$G_{T1}/G_{T2} = \left(\theta_{T2}^2/\theta_{T1}^2\right)\exp\left[-2(\delta\theta)^2\left(1/\theta_{T1}^2 - 1/\theta_{T2}^2\right)\right] \tag{48}$$

assuming the beam intensity profile is Gaussian. The only unknown parameter in these two relations is the pointing variance. In practice, of course, changing the beam divergence between two accurately known values during a single pass can be technically challenging and would probably upset the laser system calibrations needed for precise ranging. However, if the objective is only to estimate effective pointing variance, then precise range measurements on the order of a centimeter may not be needed. Even slant ranges computed from the nominal target ephemeris should be sufficiently accurate.

VI. Conclusions

In this paper a linearized error analysis has been developed to compare methods of calibration of the Naval Space Surveillance System (Fence). It has been verified that postfit satellite ephemerides derived from high-precision laser-ranging data can produce a calibration precision, over a wide range of satellite altitudes, that is well below the present noise floor of the Fence-measured direction cosines. In previous work it was found empirically that the level of cosine error estimated to be resolvable by the ephemeris method was below the noise floor of 10 μrad at zenith. In the present work these results are confirmed analytically. Simple geometric measurement models have been used to derive explicit formulas relating the precision of calibration reference data to the smallest resolvable direction-cosine errors for the Fence. The analysis includes the effects of pass geometry, ephemeris position uncertainty, and Fence station location uncertainty on the calibration precision. It was found that zenith passes over a Fence station whose data is to be calibrated produces the worst-case calibration precision, on average, over many randomly distributed passes. This fact allows ephemeris-based calibration requirements to be approximated by a very simple formula [Eq. (19)].

Also examined is a method of calibrating Fence direction cosines by direct comparison with simultaneous laser ranging data. Specifically, if a sufficiently precise three-dimensional position of a satellite can be computed directly from SLR ranges and telescope angles measured as the satellite crosses the Fence, then one can consider a near real-time comparison of Fence data with simultaneous SLR data, without the complexities of high-precision orbit determination. In this method the attainable calibration precision is strongly dependent on pass geometry at both the laser station and the Fence station, and no general "worst case" is apparent. The implication is

that simultaneous-track calibration has to be carefully planned and suitable passes selected well in advance of the data collection. When only the total angular measurement uncertainty of the laser ranging system is considered, that uncertainty is found to be directly proportional to the smallest resolvable direction cosine uncertainty. The proportionality factor contains all of the effects of pass geometry at both stations and provides a convenient scalar criterion for accepting or rejecting a candidate pass for simultaneous-track calibration. Some insight has been gained into the question of how important it is to have the SLR calibrator co-located with a Fence receiver in order to do simultaneous-track calibration. Numerical results with both real and simulated satellite passes indicate that it is co-location with respect to the Fence plane rather than to the receiver sites themselves that provides more opportunities for sufficiently precise calibration.

The simultaneous-track approach to Fence calibration raises the question of how well SLR systems can measure positions in space. The ability of most laser ranging systems to estimate three-dimensional satellite position directly (without orbit determination) is limited by the total angular measurement precision. In turn, the total angular measurement precision is usually dominated by uncertainties caused by the beam divergence angle. For a laser-ranging system having fixed boresight pointing uncertainty and a Gaussian beam intensity profile, there is an optimum value of beam divergence that maximizes the gain, or, equivalently, the detectable number of photons. At the gain-optimum value of beam divergence, the total angular measurement variance is three times the boresight pointing variance. For beam divergence values above the gain-optimum value, one can improve both the gain and the total angular measurement uncertainty by reducing the beam divergence. For beam divergences below the gain-optimum value, the total angular measurement uncertainty can still be reduced by decreasing the beam divergence but at the cost of lower gain. Consequently, for a given laser-ranging system, the achievable total angular measurement precision is fixed by the combination of boresight pointing uncertainty and lowest usable transmitter gain.

References

[1] Gilbreath, G. C., Schumacher, P. W., Jr., Davis, M. A., Lydick, E. D., and Anderson, J. M., "Evaluation of the Naval Space Surveillance Fence Performance Using Satellite Laser Ranging," *Journal of Guidance, Control, and Dynamics*, Vol. 22, No. 1, 1999, pp. 149–155.

[2] Coffey, S. L., Neal, H. L., Visel, C. L., and Conolly, P. C., "Demonstration of Special Perturbations-Based Catalog in the Naval Space Command System," *Advances of the Astronautical Sciences*, Vol. 99, American Astronautical Society, Springfield, VA, 1998, pp. 225–248.

[3] Schumacher, P. W., Jr., Gilbreath, G. C., Lydick, E. D., Walters, S. G., Davis, M. A., and Seago, J. H., "Design for Operational Calibration of the Naval Space Surveillance System," *Advances in the Astronautical Sciences*, Vol. 99, American Astronautical Society, Springfield, VA, Pt. 1, 1998, pp. 279–295.

[4] Taylor, J. R., *An Introduction to Error Analysis*, Oxford Univ. Press, Mill Valley, CA, 1982, Chap. 3.

[5] Barlow, R. J., *Statistics*, Wiley, New York, 1989, Chap. 4.

[6] "Department of Defense World Geodetic System 1984: Its Definition and Relationships with Local Geodetic Systems," 3rd ed., NIMA TR 8350.2, U.S. Government Printing Office, Washington, DC, 4 July 1997.

[7] Gilbreath, G. C., Davis, M. A., Rolsma, P., Meehan, T., Eichinger, R., and Anderson, J. M., "NRL@SOR: Satellite Laser Ranging with Robust Links," *Society of Photo-Optical Instrumentation Engineers Proceedings*, Vol. 3065, Society of Photo-Optical Instrumentation Engineers, Bellingham, WA, 1997, p. 116.

[8] Degnan, J. J., "Millimeter Accuracy Satellite Laser Ranging: A Review," *Contributions of Space Geodesy to Geodynamics: Technology*, Geodynamics Series, Vol. 25, American Geophysical Union, Washington, DC, 1993, pp. 133–162.